

In vivo carotid artery closure by laser activation of hyaluronan-embedded gold nanorods

Paolo Matteini

Fulvio Ratto

Francesca Rossi

Institute of Applied Physics "Nello Carrara"
Italian National Research Council
via Madonna del Piano, 10
50019 Sesto Fiorentino, Italy

Giacomo Rossi

University of Camerino
Faculty of Veterinary Medicine
via Circonvallazione, 93/95
62024 Matelica, Italy

Giuseppe Esposito

Alfredo Puca

Alessio Albanese

Giulio Maira

Catholic University School of Medicine
Institute of Neurosurgery
L.go A. Gemelli, 8
00168 Rome, Italy

Roberto Pini

Institute of Applied Physics "Nello Carrara"
Italian National Research Council
via Madonna del Piano, 10
50019 Sesto Fiorentino, Italy

Abstract. We prove the first application of near-infrared-absorbing gold nanorods (GNRs) for *in vivo* laser closure of a rabbit carotid artery. GNRs are first functionalized with a biopolymeric shell and then embedded in hyaluronan, which gives a stabilized and handy laser-activable formulation. Four rabbits undergo closure of a 3-mm longitudinal incision performed on the carotid artery by means of a 810-nm diode laser in conjunction with the topical application of the GNRs composite. An effective surgery is obtained by using a 40-W/cm² laser power density. The histological and electron microscopy evaluation after a 30-day follow-up demonstrates complete healing of the treated arteries with full re-endothelization at the site of GNRs application. The absence of microgranuloma formation and/or dystrophic calcification is evidence that no host reaction to nanoparticles interspersed through the vascular tissue occurred. The observation of a reshaping and associated blue shift of the NIR absorption band of GNRs after laser treatment supports the occurrence of a self-terminating process, and thus of additional safety of the minimally invasive laser procedure. This study underlines the feasibility of using GNRs for *in vivo* laser soldering applications, which represents a step forward toward the introduction of nanotechnology-based therapies in minimally invasive clinical practices. © 2010 Society of Photo-Optical Instrumentation Engineers. [DOI: 10.1117/1.3449574]

Keywords: laser soldering; gold nanorods; photothermal effects; hyaluronan.

Paper 09459SSR received Oct. 10, 2009; revised manuscript received Mar. 1, 2010; accepted for publication Apr. 9, 2010; published online Jul. 6, 2010.

1 Introduction

Photothermal laser welding is a technique used to seal accidental or surgical wounds. It exploits the interaction of laser light with an optical absorber, which can be endogenous as body water or exogenous as an organic dye, to transduce the laser light into heat.^{1,2} When the weld is mediated by the topical interposition of a laser-activated material (solder), this technique is typically referred to as laser soldering. Over the last decade, the combination of near-infrared (NIR) radiation, which penetrates deep into the body, with an exogenous chromophore such as indocyanine green (ICG) has improved critical aspects of previous laser welding and soldering approaches, including collateral tissue overheating and lack of selectivity.³⁻⁵ However, despite the significant experimental and clinical achievements of the last few years, some limitations still hinder a standardized clinical application of this technology. The principal limitations are ascribed to the use of organic dyes, which exhibit poor photochemical stability, excessive diffusiveness in the biological environment, and inadequate stability when stored in an aqueous solution or dis-

persed in a physiological environment.² This jeopardizes the sustainability of the product and the efficacy of the photothermal conversion.

Substantial breakthrough in the laser welding (and soldering) of biological tissues may come from the advent of nanotechnologies. Recent advances in colloidal chemistry have driven the design of nanoparticles with excellent optical response, which hold the potential to outclass the organic dyes presently in use. One relevant example is hybrid materials as organic or inorganic nanoparticles embedded with ICG, which becomes relatively protected and stabilized in the biological environment.⁶ Another innovative example are metal oxide and metal nanoparticles with magnetic and plasmonic resonances, respectively, which may provide high efficiency and localization of heat release. Recent reports have described experimental tests on the use of electromagnetically excited iron oxide nanospheres⁷ and laser-activated gold nanoshells⁸ to seal arteries and skin, respectively. Among the other metal nanoparticles, gold nanorods (GNRs) appear an ideal candidate to replace the organic dyes in use.^{9,10} These are cylindrical gold nanoparticles with plasmon absorption bands in the NIR window, which can be tuned by a controllable modulation of their size and shape.¹¹ Remarkable features of these

Address all correspondence to: Paolo Matteini, Institute of Applied Physics "Nello Carrara", Italian National Research Council, via Madonna del Piano, 10-Sesto Fiorentino, 50019 Italy; Tel: 0039 055 5225307; Fax: 0039 055 5225305; E-mail: p.matteini@ifac.cnr.it

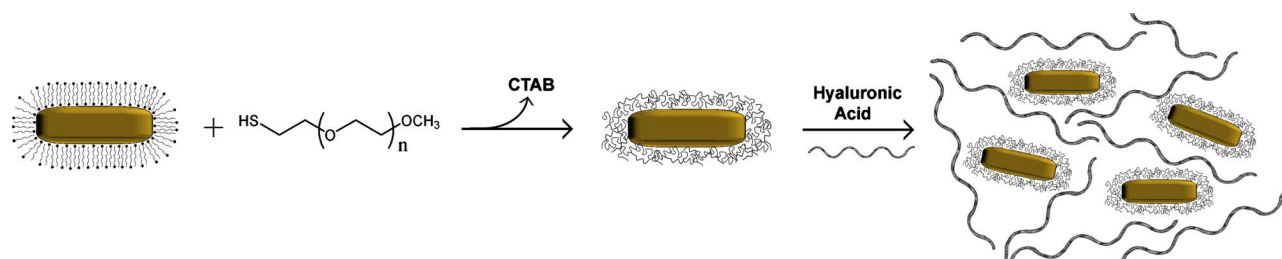


Fig. 1 Scheme of the steps followed in the synthesis of the GNRs-HA composite.

nanoparticles include exceptional optical absorption and excellent biochemical versatility and stability under physiological conditions, as well as high laser irradiances.¹⁰ In addition, their lower diffusivity through the tissue matrix with respect to that of organic dyes (e.g., $\sim 10^{-8} \text{ cm}^2 \text{ s}^{-1}$ for $\sim 100\text{-nm}$ gold nanoparticles¹² compared with $\sim 10^{-6} \text{ cm}^2 \text{ s}^{-1}$ for indocyanine green through connective tissues¹³) provides for better localization of the photothermal conversion, which translates into a minimization of overheating problems and optimization of efficiency and selectivity.¹⁴ The probable biocompatibility of these nanoparticles represents another attraction, which justifies the intense interest in these new materials for several biomedical applications.

Recently, we reported the use of a solution of GNRs in the direct welding of sandwiches of lens capsular tissues obtained from porcine eyes *ex vivo*.¹⁴ These results provided the first proof of the capacity of laser-activated GNRs to mediate substantial and functional photothermal effects in a model connective tissue. In this work, we report the first application of GNRs for *in vivo* laser closure of a rabbit carotid artery. GNRs were functionalized with a biopolymeric shell and then embedded in a hyaluronan viscous solution to achieve a highly stabilized and handy material, suitable for manipulation by the surgeon. In addition, the choice of hyaluronan offers the advantage of well-known physiochemical and biological properties,¹⁵ which makes it a unique solution for the preparation of new biocompatible and biodegradable composites for wound repair purposes.¹⁶

2 Experimental Section

2.1 Materials

All chemicals were purchased from Sigma-Aldrich (Saint Louis, Missouri) unless otherwise noted and used without further purification. Methoxypoly-(ethylene glycol) (mPEG-SH) with a 5000-Da mass was supplied by Laysan Bio Incorporated (Arab, Alabama). We used hyaluronan obtained from a bacterial source to minimize possible protein-mediated aggregation of polymer chains when storing for long times in aqueous solutions. In particular, hyaluronan sodium salt from *Streptococcus equi* (Esperis S.p.A., Milan, Italy) having a molecular mass of approximately 1000 kDa and with a protein content lower than 0.025%, as previously measured,¹⁵ was used in the experiment.

2.2 Synthesis of the Gold Nanorod Hyaluronic Acid Formulation

The exogenous chromophore consisted of a gel-like paste of functionalized GNRs (Fig. 1). In brief, colloidal suspensions of GNRs were obtained by the seed-mediated surfactant-assisted (cetrimonium bromide or CTAB) reduction of chloroauric acid by ascorbic acid (according to a variant of the Nikoobakht method; see Ref. 14 for details). As-grown GNRs were further subjected to overgrowth by implementation of a protocol recently developed by our group.¹¹ This allowed us to achieve a 100-pM aqueous suspension of 25-nm average diameter \times 102-nm average length GNRs (aspect ratio ~ 4) (Fig. 2, left inset). The solution was then concentrated to 800 pM by centrifugation and redispersed into water, showing enhanced absorption in the NIR (see Fig. 2, solid line), with a measured absorption coefficient at 810 nm of about 16 cm^{-1} . The surfactant bilayer that coats the GNRs was replaced by mPEG-SH to make the nanoparticles stable in a physiological solution and ready for the following dispersion in the hyaluronan matrix. The substitution was carried out by a previously described protocol.¹⁷ In brief, 0.2 ml of 10^{-3} M mPEG-SH and 0.1 ml of $2 \cdot 10^{-3} \text{ M}$ K_2CO_3 were added to 1-ml GNRs suspension. The mixture was set overnight at

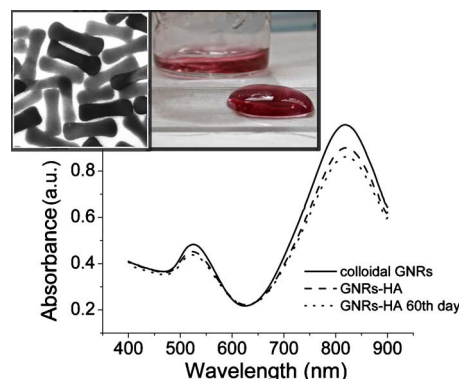


Fig. 2 Comparison among the optical absorbances of the colloidal GNRs suspension (solid line) of the GNRs-HA formulation at the time of the synthesis (dashed line) and after 60 days of storage at daylight and room temperature (dotted line). Common characteristics are the longitudinal band in the NIR (at $\sim 820 \text{ nm}$) and the transversal band in the visible (at $\sim 530 \text{ nm}$). Inset: (left) $236 \times 236\text{-nm}^2$ transmission electron micrograph of the gold nanorods used in the tests (aspect ratio=4), and (right) appearance of the GNRs-HA composite.

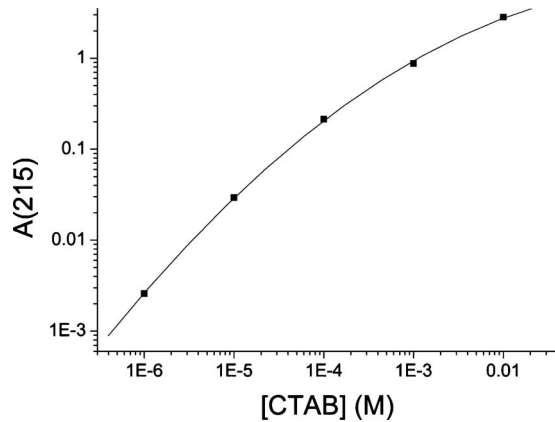


Fig. 3 Calibration curve relating the concentration of aqueous solutions of CTAB with the 215-nm absorbance response.

room temperature, centrifuged, and resuspended in distilled water two times to remove the replaced CTAB and the excess mPEG-SH.

2.3 Measure of the Residual Cetrimonium Bromide

Since CTAB is cytotoxic, its presence in the batch used for the fabrication of the GNRs-HA solder needed to be quantified. After pegylation and washing, the residual CTAB contained in the GNRs solution (1 ml) was extracted into chloroform as reported in the literature.¹⁸ We carried out two extraction cycles by using a total of 3-ml chloroform. The organic phases were combined and left to evaporate at room temperature, and the dry residual was dispersed again in 1 ml of pure water. The absorbance of the sample at 215 nm [A(215)] was considered for the quantification of the CTAB present in the sample,¹⁹ on comparison with a calibration curve of CTAB aqueous solutions in the $10^{-2} \div 10^{-6}$ M range (Fig. 3). Using this procedure, we found a residual CTAB not above the detection limit of our method (i.e., $\sim 10^{-6}$ M) (average of three replicates), which is below the 50% inhibitory concentration (IC₅₀) of CTAB ($9.1 \cdot 10^{-6}$ M), as previously reported.¹⁸ This insight suggests a negligible toxicity of our pegylated GNRs, which are thus regarded as potentially safe for use *in vivo*.

2.4 Preparation of the Gold Nanorod Hyaluronic Acid Formulation

The pegylated nanoparticles were centrifuged and suspended in phosphate buffered saline (PBS, pH 7.4, 0.1-M phosphate buffer, 0.15-M NaCl). Hyaluronan was added to the suspension until a final 3% (w/v) concentration was reached. The mixture (referred to hereafter as GNRs-HA) was gently shaken for two days to obtain a homogeneous dark-red transparent paste (Fig. 2, right inset), which was stable at room temperature for at least a four-months period without significant modifications of its optical properties (Fig. 2, dotted line).

2.5 Surgical Procedure

The surgeries were performed on four rabbits in the vivarium of the Catholic University in Rome. The animals were anesthetized with ketamine hydrochloride (50 mg/kg) and me-



Fig. 4 Sequence of images recorded during the laser welding procedure. (a) The artery is clamped and a 3-mm longitudinal incision is performed. (b) After the application of the GNRs-HA formulation, the incision is treated with the diode laser light. (c) Appearance of the sealed artery immediately after intervention.

detomidine (0.3 mg/kg) intramuscularly. During the follow-up period, the animals were treated with antibiotics (10 mg/kg of enrofloxacin per day). Protocols of animal tests were designed according to the recommendation and regulation of the Italian Ministry of Health.

The laser used in the tests was an AlGaAs diode laser (model WELD 800 by El.En. SpA, Calenzano, Italy) emitting at 810 nm and equipped with a 200- μ m-diam optical fiber terminating in a hand piece to enable easy operation.

After the anaesthesia, a 3-cm segment of the right common carotid artery was dissected and then clamped proximally and distally. The laser surgery consisted of the closure of 3-mm longitudinal cuts previously executed along the artery, which represents a clinically relevant situation in neurosurgery.²⁰⁻²² Prior to laser irradiation, a total quantity of ~ 10 mg of GNRs-HA formulation was first applied above and inside the cut by means of a spatula. Then excess material was immediately removed, which resulted in a residual 5 to 20- μ m-thick solder layer on the artery surface. This operation was performed with the aid of a surgical microscope to avoid entrance of solder material into the lumen, and consequently, to confine the photothermal effect to the vascular surface. Laser irradiation of the cuts was then performed by slowly moving the fiber tip, held at a constant distance of 2 to 3 mm from the tissue. A continuous laser power (out of the fiber) of 0.6 W, corresponding to a power density of 40 W/cm² at the surface of the artery, and an average time exposure ≈ 15 to 20 s were found to induce an effective closure of the cut edges. Control tests performed with the same laser parameters and blank hyaluronan failed to induce any detectible photothermal effect nor wound closure. Upon clamp removal immediately after the surgery, no bleeding was observed from the laser-soldered cuts (see Fig. 4). At the end of the procedure, the carotid patency was verified by Doppler analysis, the artery was closed in layers, and the animal was left to recover from the anaesthesia.

2.6 Histological Evaluation after Follow-Up

After a follow-up period of 30 days, the animals ($n=4$) were examined and reanesthetized. After animal sacrifice, artery specimens including the laser-treated segment were excised and treated following standard pathology laboratory procedures for the histological evaluation. In brief, the samples were fixed in 10% buffered formalin and embedded in paraffin. Semi-thin (3 μ m) sections were obtained by cutting the paraffin-embedded samples with a microtome (model RM2235, Leica Microsystems GmbH, Germany). The final geometry of the sections included both the treated superficial and adventitial portion of the vessel wall in the central area, and the two hemilines of the endothelium at the periphery. To obtain this geometry, we isolated the treated area of the ves-

sel, opened the vessel, and operated a superficial longitudinal cut along the laser-treated line to comprise the endothelial, subendothelial, muscular, and partially, adventitial stratum of the vessel wall. The so-obtained samples were then embedded in a shallow block of paraffin by laying them flat and finally sliced. The slices were laid onto electrostatically charged slides (Superfrost®, Histoline, Milan, Italy) and left overnight with a thermostat at 38 °C. Then, after deparaffinization and rehydration, the sections were stained with hematoxylin and eosin, van Gieson's stain for collagen and elastic fibres, and Masson's trichrome stain for connective tissue. Additionally, tissue sections were immunohistochemically tested for the presence of CD31 and von Willebrand factor (vWF) by use of a monoclonal mouse antihuman CD31 and a mouse antihuman factor VIII antibodies (DAKO, Glostrup, Denmark), respectively. Immunostaining was performed with a biotinylated secondary antibody (Vectastain ABC kit, Vector Laboratories, Burlingame, California) and diaminobenzidine-HCl (Vector). Other samples were fixed in 2.5% glutaraldehyde, postfixed with 1% osmium tetroxide, and infiltrated in epoxy resin. Ultrathin sections of 60 nm were contrasted with uranyl acetate and lead citrate, and inspected under a transmission electron microscope operating at 80 kV.

2.7 Characterization of the Morphological and Optical Changes of Gold Nanorods upon Laser Irradiation

The effect induced by laser irradiation to the nanoparticles was studied in detail. A small amount (~10 mg) of GNRs-HA gel was spread onto a small (1 cm diameter) glass dish to obtain a thin layer on the order of 10 to 20 μm. In an attempt to simulate the surgical environment, some drops of PBS were added in such a way that the liquid could only wet the gel borders. The laser treatment of the sample was achieved by delivering laser light of 40-W/cm² power density obtained by keeping the 200-μm fiber tip fixed at a distance of 2.5 mm from the sample surface (in a similar way to a previous experimental setup²³) in accordance with a standard laser soldering procedure. The irradiation time was fixed to 5 s, which is a good approximation of the operative time needed by the surgeon to obtain an effective photothermal effect (this time is referred to a ~1.4-mm irradiated spot by considering a 0.24 fiber numerical aperture). The experiment was repeated by irradiating different areas of the sample for double and quadruple the time (10 and 20 s) to investigate the effect of overirradiation of the sample.

After irradiation, the samples were subject to spectromicroscopy by a homemade setup²⁴ composed of a transmission microscope (model DM 2500 by Leica Microsystems GmbH, Germany), a visible-NIR spectrometer (model EPP200 by Stellarnet Incorporated, Tampa, Florida) and a set of interchangeable high-pass filters. The visible and NIR windows were examined under different conditions to optimize the signal detection.

Afterward, samples (including also an untreated region used as a control) were carefully removed from the dishes, resized, placed onto copper grids, contrasted with uranyl acetate and lead citrate, and finally analyzed by transmission electron microscopy (TEM).

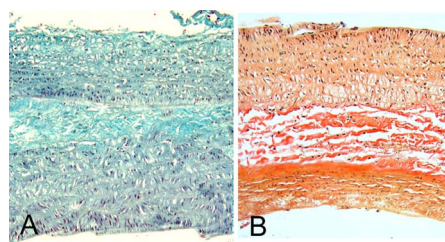


Fig. 5 Histochemical results demonstrating a good preservation of the carotid wall after laser soldering. Note the typical physiological pattern maintained by collagen and elastic fibers. The central laser-treated area is characterized by a bright blue or dark orange color during staining with (a) Masson's trichrome and (b) Van Gieson, respectively. (Color online only.)

3 Results and Discussion

All the laser-soldered arteries were found to be patent at the end of the 30-day follow-up period. Histology on operated samples demonstrated substantial integrity of the vascular wall at the site treatment, with no damage to the *tunica elastica externa*, nor observable collagen homogenization [Figs. 5(a) and 5(b)]. The absence of microgranuloma formation and/or dystrophic calcification of the vasal media and/or intima showed that no host reaction to nanoparticles interspersed throughout the treated vascular tissue occurred.

Immunohistochemical results showed the integrity and viability of the endothelium with a constant and intense expression of CD31 and vWF [Figs. 6(a) and 6(b)]. This suggests that the introduction of the GNRs-HA formulation in laser welding surgeries may give substantial control over laser dosimetry, which is critical to avoid thrombogenic effects during the wound healing period. Interestingly, these results improve previous findings when a conventional chromophore, i.e., ICG, was used to seal rabbit vessels.³ In summary, we achieved conspicuous photothermal effects, which were able to induce local tissue fusion while preserving the endothelial viability and preventing thermally induced thrombogenicity.

TEM micrographs of the laser-treated site showed spherical nanoparticles interdispersed among intact collagen fibers (Fig. 7), which indicates a morphological remodeling of the GNRs. This finding suggests the possibility of a self-termination of the laser soldering process. Indeed, the blue shift of the absorption spectrum of the GNRs associated with their thermally activated transformation into more stable shapes may inhibit further laser power absorption and photothermal conversion. The possibility that the solder may undergo a self-terminating process during the surgery was studied in some detail by carrying out focused bench experiments,

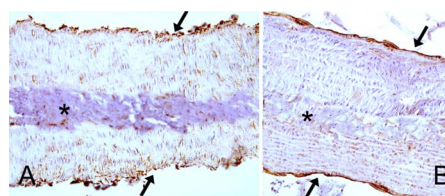


Fig. 6 Immunohistochemistry of laser-treated vessels: (a) vWF and (b) CD31 good expression by the endothelium (arrows) over the treated area (*), indicating preservation of endothelial viability.

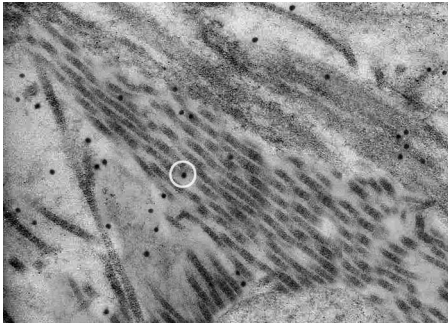


Fig. 7 TEM micrograph ($4.2 \times 3.0 \mu\text{m}^2$) of the weld site. Approximately 40-nm spherical nanoparticles (as the one indicated by a circle) are visible, interspersed among intact collagen fibers, indicating a rod-to-sphere reshaping.

as introduced in Sec 2. The optical properties of GNRs-HA films subject to different laser irradiation times at constant power density (40 W/cm^2) were investigated by optical spectromicroscopy and electron microscopy. The spectral analysis evidenced a consistent blue shift of the longitudinal band originally peaked at $\sim 820 \text{ nm}$ to a final $\sim 660 \text{ nm}$ [Fig. 8(a)]. The wavelength position of this new band and its integrated intensity ratio to the transversal band at 530 nm proved comparable for all the samples (5-, 10-, and 20-s irradiation), as summarized in Fig. 8(b). TEM analysis of the control sample revealed $(102 \pm 3) \text{ nm}$ in length \times $(25 \pm 2) \text{ nm}$ in diameter (aspect ratio ~ 4.0) GNRs well spread within a regular hyaluronan matrix and never assembled in clusters [Fig. 9(a)]. This result supports the spectrophotometric analysis of the GNRs-HA gel summarized in Fig. 2, which indicated a substantial preservation of the optical properties of the nanoparticles after pegylation and inclusion in the hyaluronan gel. The TEM micrographs of the 5-s irradiated sample showed $(66 \pm 14) \text{ nm}$ in length \times $(31 \pm 7) \text{ nm}$ in diameter fat GNRs (aspect ratio ~ 2.1) dispersed in a blurred and spotted hyaluronan network. This sample was then compared to the films irradiated for double and quadruple the time (10 and 20 s). No detectable difference in the average nanoparticle size nor evident changes in the hyaluronan matrix were observed [see Fig. 9(b)], confirming that the remodeling of GNRs and modification of bulk HA were essentially negligible after additional

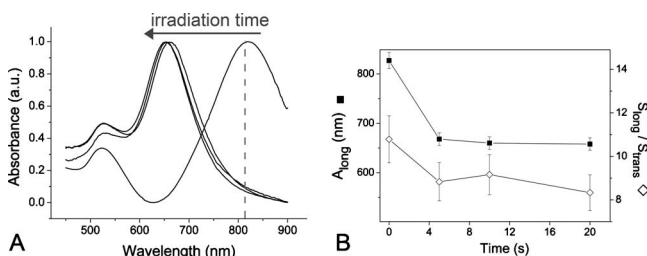


Fig. 8 (a) Change of the optical properties of the untreated and laser-treated GNRs-HA films (considered irradiation times are 5, 10, and 20 s) showing a blue shift of the longitudinal absorbance band at 820 to 660 nm on NIR laser treatment (laser emission is indicated with a dashed line). (b) Variation of the position of the longitudinal band (A_{long}) and of the integrated intensity ratio between the longitudinal and transversal bands ($S_{\text{long}}/S_{\text{trans}}$) with irradiation time.

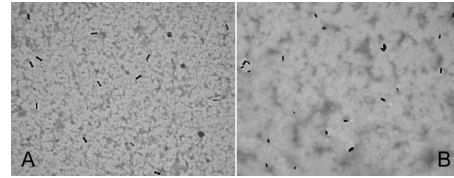


Fig. 9 TEM micrographs ($3.3 \times 2.6 \mu\text{m}^2$) of (a) untreated and (b) 20-s laser-treated GNRs-HA films.

5 or 15 s of laser irradiation. Identical effects were also observed at different output powers (at least within a factor of 2) and hydration conditions, which were tested to challenge the possibility to translate our observations. The blue shift of the longitudinal band is in good agreement with the rounding of the rods, as detected by TEM analysis.²⁵ These observations imply a drastically reduced possibility of NIR photothermal conversion, which in turn supports the occurrence of a self-terminating process during the laser soldering procedure with the GNRs-HA nanocomposite, thus corroborating the previously formulated speculations. The partial remodeling of GNRs observed in this bench experiment is apparently in partial disagreement with the TEM analysis of the treated rabbit arteries after the 30-day follow-up, as displayed in Fig. 7, which reveals $(40 \pm 2) \text{ nm}$ in diameter nanospheres (highly monodispersed) within the connective matrix. We suggest that the complete rod-to-sphere change of the GNRs can effectively conclude during the 30-day wound healing of the artery, which is well presumable in consideration of the kinetic behavior of GNR remodeling,²⁶ which may slowly develop at a physiological temperature (37°C) (though being much more rapid on laser activation in the millisecond time scale).

4 Conclusions

In our previous work, we had reported the ability of a colloidal GNR suspension to induce conspicuous thermal effects, which led to local tissue fusion in porcine lens capsules excised *ex vivo*.¹⁴ Here we confirm *in vivo* the potential of the laser technique performed by laser activation of a semisolid and biocompatible formulation of GNRs. First, the dispersion of the GNRs into the hyaluronan matrix provides better manipulation and a highly stabilized product, which can be easily stored with minimal optical and structural modifications over time. Second, the low diffusivity of gold nanoparticles allows us to minimize collateral overheating and to increase the selectivity of the treatment, as revealed by the substantial preservation of the endothelium and inner wall structures of arteries. Third, the complete absence of a host reaction after a 30-day follow-up is encouraging toward a good biocompatibility of the GNR formulation, which is further supported by the negligible residual CTAB detected in the GNR solution used to fabricate the gel. Fourth, interestingly, GNRs undergo conspicuous reshaping on laser irradiation, which suggests the possibility of a self-terminating process and thus of additional safety of the minimally invasive laser procedure. Overall, this work highlights the feasibility of *in vivo* laser soldering operations by means of NIR-absorbing GNRs. This outcome represents an advancement toward the introduction of GNRs in clinical practice, which will require further investigation to

solve critical questions raised by the use of metal nanoparticles, such as their sustainability and metabolism dynamics.

References

1. K. M. McNally, "Laser tissue welding," Chap. 39, in *Biomedical Photonics Handbook*, T. Vo-Dihn, Ed., pp. 1–45, CRC Press, Boca Raton, FL (2003).
2. R. Pini, F. Rossi, P. Matteini, and F. Ratto, "Laser tissue welding in minimally invasive surgery and microsurgery," in *Biophotonics. Series: Biological and Medical Physics, Biomedical Engineering*, L. Pavese and P. M. Fauchet, Eds., pp. 275–299, Springer, Berlin (2008).
3. A. Puca, A. Albanese, G. Esposito, G. Maira, B. Tirpakova, G. Rossi, A. Mannocci, and R. Pini, "Diode laser-assisted carotid bypass surgery: an experimental study with morphological and immunohistochemical evaluations," *Neurosurgery* **59**(6), 1286–1295 (2006).
4. S. D. DeCoste, W. Farinelli, T. Flotte, and R. R. Anderson, "Dye-enhanced laser welding for skin closure," *Lasers Surg. Med.* **12**(1), 25–32 (1992).
5. F. Rossi, R. Pini, L. Menabuoni, R. Mencucci, U. Menchini, S. Ambrosini, and G. Vannelli, "Experimental study on the healing process following laser welding of the cornea," *J. Biomed. Opt.* **10**(2), 024004 (2005).
6. V. Saxena, M. Sadoqi, and J. Shao, "Indocyanine green-loaded biodegradable nanoparticles: preparation, physicochemical characterization and *in vitro* release," *Int. J. Pharm.* **278**, 293–301 (2004).
7. M. Reinert, A. Bregy, A. Kohler, B. Steitz, A. Petri-Finkb, S. Bogni, A. Alfieri, M. Munker, I. Vajtai, M. Frenz, and H. Hofmann, "Electromagnetic tissue fusion using superparamagnetic iron oxide nanoparticles: first experience with rabbit aorta," *Open Surg. J.* **2**, 3–9 (2008).
8. A. M. Gobin, D. P. O'Neal, D. M. Watkins, N. J. Halas, R. A. Drezek, and J. L. West, "Near infrared laser-tissue welding using nanoshells as an exogenous absorber," *Lasers Surg. Med.* **37**(2), 123–129 (2005).
9. M. Hu, J. Chen, Z. Y. Li, L. Au, G. V. Hartland, X. Li, M. Marqueze, and Y. Xia, "Gold nanostructures: engineering their plasmonic properties for biomedical applications," *Chem. Soc. Rev.* **35**, 1084–1094 (2006).
10. P. K. Jain, K. S. Lee, I. H. El-Sayed, and M. A. El-Sayed, "Calculated absorption and scattering properties of gold nanoparticles of different size, shape, and composition: applications in biological imaging and biomedicine," *J. Phys. Chem. B* **110**, 7238–7248 (2006).
11. F. Ratto, P. Matteini, F. Rossi, and R. Pini, "Size and shape control in the overgrowth of gold nanorods," *J. Nanopart. Res.* (2009).
12. G. Sonavane, K. Tomoda, A. Sano, H. Ohshima, H. Terada, and K. Makino, "In vitro permeation of gold nanoparticles through rat skin and rat intestine: effect of particle size," *Colloids Surf. B Biointerfaces* **65**, 1–10 (2008).
13. E. A. Genina, M. Y. Kuzmina, S. S. Pankov, A. N. Bashkatov, and V. V. Tuchin, "In vitro study of indocyanine green solution interaction with skin," *Proc. SPIE* **6535**, 65351H (2007).
14. F. Ratto, P. Matteini, F. Rossi, L. Menabuoni, N. Tiwari, S. K. Kulkarni, and R. Pini, "Photothermal effects in connective tissues mediated by laser-activated gold nanorods," *Nanomed. Nanotechnol. Biol. Med.* **5**, 143–151 (2009).
15. P. Matteini, L. Dei, E. Carretti, N. Volpi, A. Goti, and R. Pini, "Structural behavior of hyaluronan under high concentration conditions," *Biomacromolecules* **10**, 1516–1522 (2009).
16. W. Y. J. Chen and G. Abatangelo, "Function of hyaluronan in wound repair," *Wound Repair Regen* **7**, 79–89 (1999).
17. T. Niidome, M. Yamagata, Y. Okamoto, Y. Akiyama, H. Takahashi, T. Kawano, Y. Katayama, and Y. Niidome, "PEG-modified gold nanorods with a stealth character for *in vivo* applications," *J. Controlled Release* **114**, 343–347 (2006).
18. H. Takahashi, Y. Niidome, K. Kaneko, H. Kawasaki, and S. Yamada, "Modification of gold nanorods using phosphatidylcholine to reduce cytotoxicity," *Langmuir* **22**, 2–5 (2006).
19. M. Medenica, D. Ivanovic, and A. Malenovic, "Simultaneous determination of compounds in Septalen pellets by derivative spectrophotometry," *J. Serb. Chem. Soc.* **65**, 339–344 (2000).
20. N. Sanai, Z. Zador, and M. T. Lawton, "Bypass surgery for complex brain aneurysms: an assessment of intracranial-intracranial bypass," *Neurosurgery* **65**, 670–683 (2009).
21. R. A. Hanel and R. F. Spetzler, "Surgical treatment of complex intracranial aneurysms," *Neurosurgery* **62**(6 Suppl 3), 1289–1297 (2008).
22. M. T. Lawton, A. Quinones-Hinojosa, N. Sanai, J. Y. Malek, and C. F. Dowd, "Combined microsurgical and endovascular management of complex intracranial aneurysms," *Neurosurgery* **52**, 263–274 (2003).
23. P. Matteini, F. Ratto, F. Rossi, R. Cicchi, C. Stringari, D. Kapsokalyvas, F. S. Pavone, and R. Pini, "Photothermally-induced disordered patterns of corneal collagen revealed by SHG imaging," *Opt. Express* **17**, 4868–4878 (2009).
24. F. Ratto, P. Matteini, S. Centi, F. Rossi, and R. Pini, "Stability of cetrimonium and silica modified gold nanorods/polyvinyl alcohol nano-composites upon near infrared laser excitation," *Proc. SPIE* **7577**, 757716 (2010).
25. J. Pérez-Juste, I. Pastoriza-Santos, L. M. Liz-Marzán, and P. Mulvaney, "Gold nanorods: synthesis, characterization and applications," *Coord. Chem. Rev.* **249**, 1870–1901 (2005).
26. H. Petrova, J. Perez Juste, I. Pastoriza-Santos, G. V. Hartland, L. M. Liz-Marzán, and P. Mulvaney, "On the temperature stability of gold nanorods: comparison between thermal and ultrafast laser-induced heating," *Phys. Chem. Chem. Phys.* **8**, 814–821 (2006).